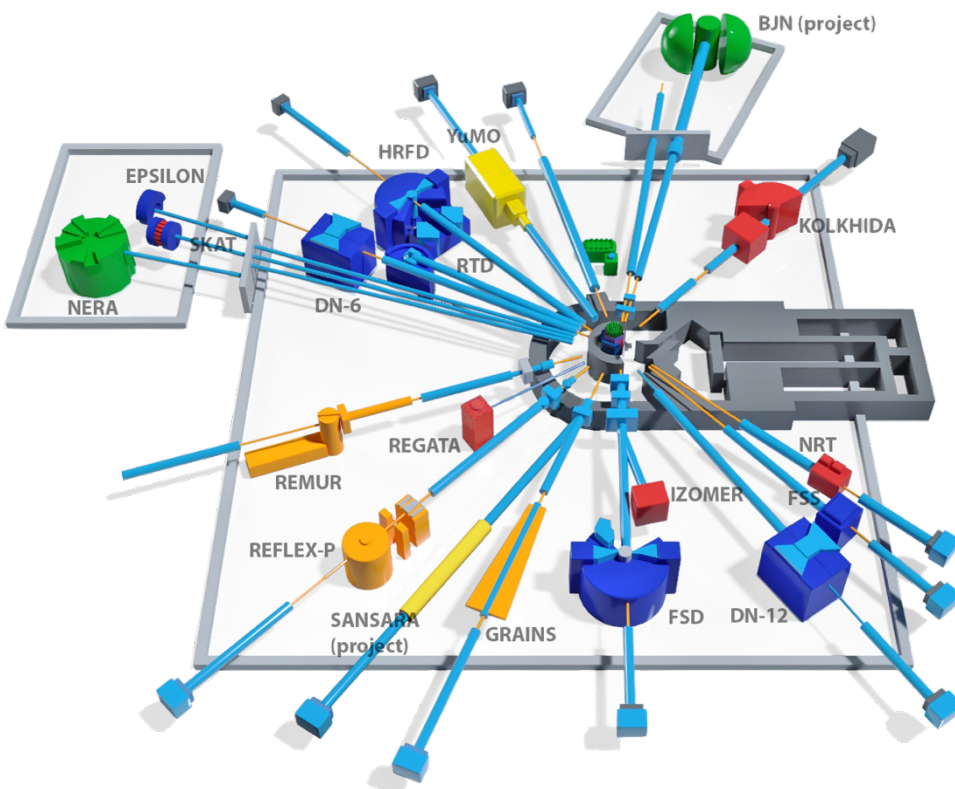


JOINT INSTITUTE FOR NUCLEAR RESEARCH

Frank Laboratory of Nuclear Physics

**FINAL REPORT ON
THE INTEREST PROGRAMME**

**INTRODUCTION TO NEUTRON
SCATTERING EXPERIMENTS AT LARGE
SCALE FACILITIES**



Student:

Bhavuk Rohilla, India

Delhi Technological University

Supervisor:

Dr. Raul Victor Erhan

Participation period:

14 June - 29 July,

Wave 7

Dubna, 2022.

Table of Contents

<i>Abstract</i>	3
<i>Acknowledgments</i>	3
Chapter A. Introduction	4
1. Neutrons	4
1.1. Neutron Property	5
1.2 Neutron Sources	5
2 X-rays	7
2.1 SAXS Small Angle X-rays Scattering	8
3. SANS Small Angle Neutron Scattering	10
3.1 Neutron time-of-flight scattering	12
Chapter B. Experimental Work By SasView	12
1. SasView Software	12
1.1 Features of SasView software	13
2. Example 1	15
2.1 Fitting with Levenberg-Marquardt and Dream algorithm	15
2.2 Using Dream Algorithm	17
3. Example 2 : Correlation Function Analysis	18
4. Example 3. P_New [SANS]	20
References	22

Abstract

Neutron scattering is a powerful tool for studying the structure and dynamics of matter over a wide range of length- and time scales. Small-angle scattering of neutron (SANS) and X-rays (SAXS) probes the statistical ensemble of the nanostructures and deal with the diffusion of electromagnetic or particle waves by heterogeneities in matter. The report contains the basic idea of SAXS and SANS with an introduction to neutron sources. In this report working of SasView software is discussed with the help of examples such as ISIS_Polymer_Blend_RT2 (mixture of polystyrenes) and ISIS_98929 (nylon-6 hydrated with D₂O).

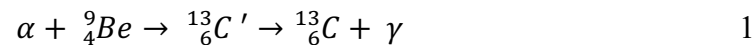
Acknowledgments

I am grateful to the people at JINR institute and the INTEREST team for organizing this programme and allowing me to participate in the same. I also need to express my deep gratitude to my supervisor **Dr Raul Victor Erhan** for giving me the chance to be a part of this project, for his teaching methods and his patience.

Chapter A. Introduction

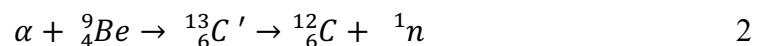
1. Neutrons

Neutron was discovered in 1932, but the experiments that led to the discovery started back in 1930 when Walther Bothe and Herbert Becker showed that the radiations emitted from beryllium when bombarded by α particle of polonium(Po) produces a radiation of great penetrating power. They correlated this with γ -rays and hypothesised that these light nuclei trap α particles, and that γ -rays release excess energy in these nuclear reactions.^[1]



In 1931 Irene Curie, Joliot and Webster conducting same experiment found that the γ radiation produced have penetrating power than any other γ -rays produced by the element and concluded that the γ -rays to be having very large energy.^[2-3]

But in 1932 James Chadwick observed something peculiar that the equation 1 does not satisfy with the energy of the radiation and mass defect of ${}^{13}\text{C}$ and that the energy of the ray produced could not be greater than $14 \cdot 10^6$ eV and proposed a new equation with a particle “Neutron”, instead of radiation having mass 1 and charge zero.^[4]



Neutrons are electrically neutral particles with a mass approximately the same as the mass of hydrogen atoms and are one of the main components of the nucleus. High-energy neutrons are emitted from chemical sources (usually AmBe or PuBe). However, neutrons can be generated in a variety of ways and can indirectly represent an important source of ionized radiation.

Neutrons are usually divided into several categories according to their energy. Thermal neutrons are neutrons that are in thermal equilibrium with material and, in special cases, have a Maxwell distribution of velocities. In this distribution, the most likely velocity at 295K is 2200m / sec, which corresponds to an energy of 0.025eV.

A neutron with an energy range of 0.5 to 10 keV is called a neutron. These neutrons are also called resonances or external thermal neutrons. Fast neutrons are neutrons in the energy range of 10 keV to 10 MeV. In this energy range, neutrons interact with material by elastic collision. Neutral neutrons whose energy exceeds 10 MeV are called relativistic neutrons.

Neutrons collide with the nuclei of forming minerals in elastic collisions. Neutrons lose the most energy when they hit the same object with the same mass, such as a hydrogen atom. A few microseconds after being emitted, the neutron loses considerable energy and enters a thermal state. In the thermal state, neutrons are captured by the nuclei of other atoms (Cl, H, B). Atoms that capture neutrons are highly excited and emit gamma rays. The tool's detector can detect epithermal neutrons, thermal neutrons, or high-energy gamma rays captured. The Compensated Neutron Tool (CNL) detects thermal neutrons and uses a percentage of the

number of short range detectors to determine porosity. The side wall neutron tool (SNP) detects epithermal neutrons and reduces the matrix effect.

1.1. Neutron Property

Neutron was once considered as one of the fundamental elementary particle but now is classified as a hadron, because it is a composite particle made of quarks. The neutron is also classified as a baryon, because it is composed of three valence quarks. The finite size of the neutron and its magnetic moment both indicate that the neutron is a composite, rather than elementary, particle. A neutron contains two down quarks with charge $-\frac{1}{3}e$ and one up quark with charge $+\frac{2}{3}e$.

Like protons, the quarks of the neutron are held together by the strong force, mediated by gluons. The nuclear force results from secondary effects of the more fundamental strong force. Like protons, the quarks of the neutron are held together by the strong force, mediated by gluons. The nuclear force results from secondary effects of the more fundamental strong force.^[5]

- **Mass** = $1.67492749804 \cdot 10^{-27}$ kg
- **Mean lifetime** = 879.4 s (free)
- **Electric charge, q_n** = zero or largest possible value is $(-0.4 \pm 1.1) \times 10^{-21} e$.
calculated by beam-deflection experiments.
- **Electric dipole moment** $< 2.9 \times 10^{-26} e \cdot \text{cm}$ (experimental upper limit)
- **Electric polarizability** = $1.16(15) \times 10^{-3} \text{ fm}^3$.
- **Magnetic moment** = $-1.91304273 \mu\text{N}$.
- **Magnetic polarizability** = $3.7(20) \times 10^{-4} \text{ fm}^3$.

1.2 Neutron Sources

A neutron source is an instrument that produces and emits neutrons that are used for various experiments. Five types of artificial neutron source are in laboratory use: radioisotope sources, photo-neutron sources, accelerator sources, nuclear reactors and spallation sources.^[9]

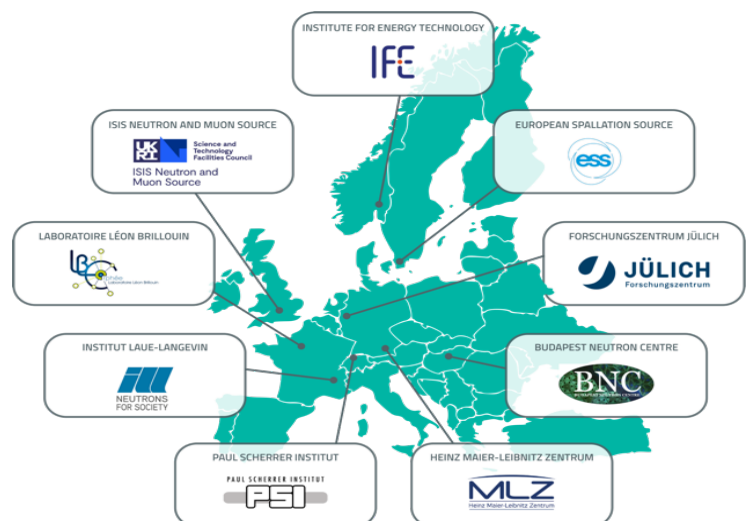


FIG 1. Neutron sources around the world

Radioisotope sources

Neutrons are produced when alpha particles hit any of several light isotopes including isotopes of beryllium, carbon, or oxygen. Thus, one can make a neutron source by mixing an alpha-emitter such as radium, polonium, or americium with a low-atomic-weight isotope, usually by blending powders of the two materials. Alpha neutron sources typically produce ~10⁶–10⁸ neutrons per second. An alpha-beryllium neutron source may produce about 30 neutrons per 10⁶ alpha particles. The useful lifetime for such sources depends on the half-life of the radioisotope. The size and cost of these neutron sources are comparable to spontaneous fission sources. Usual combinations of materials are plutonium-beryllium (PuBe), americium-beryllium (AmBe), or americium-lithium (AmLi).^[10]

Photo-neutron sources

Neutrons are produced when photons above the nuclear binding energy of a substance are incident on that substance, causing it to undergo giant dipole resonance after which it either emits a neutron (photo-neutron) or undergoes fission (photo-fission). The number of neutrons released by each fission event is dependent on the substance. Typically photons begin to produce neutrons on interaction with normal matter at energies of about 7 to 40 MeV, which means that radiotherapy facilities using megavoltage X-rays also produce neutrons, and some require neutron shielding.[citation needed] In addition, electrons of energy over about 50 MeV may induce giant dipole resonance in nuclides by a mechanism which is the inverse of internal conversion, and thus produce neutrons by a mechanism similar to that of photo-neutrons.^[10]

Nuclear fission reactors

Here neutrons are released by the fission of uranium-235. Each fission event releases 2 - 3 neutrons, though one of these is needed to sustain the chain reaction. Nuclear fission within a reactor, produces many neutrons and can be used for a variety of purposes including power generation and experiments. Research reactors are often specially designed to allow placement of material samples into a high-neutron-flux environment. The most powerful of the reactor neutron sources in the world today is the 55 MW HFR (High-Flux Reactor) at the Institute Max von Laue - Paul Langevin (ILL) in Grenoble, France. The ILL is jointly operated by France, Germany, the United Kingdom, and 12 other countries. The facility commenced operation in 1972.

Nuclear fusion systems

Nuclear fusion, the fusing of heavy isotopes of hydrogen, also has the potential to produce large numbers of neutrons. Small scale fusion systems exist for (plasma) research purposes at many universities and laboratories around the world. A small number of large scale fusion experiments also exist including the National Ignition Facility in the US, JET in the UK, and soon the ITER experiment currently under construction in France. None are yet used as neutron sources.

Inertial confinement fusion has the potential to produce orders of magnitude more neutrons than spallation. This could be useful for neutron radiography which can be used to locate

hydrogen atoms in structures, resolve atomic thermal motion and study collective excitation of nuclei more effectively than X-rays.

Spallation source

A spallation source is a high-flux source in which protons that have been accelerated to high energies hit a target with large mass number (i.e more neutrons in nucleus) , prompting emission of neutrons. The world's strongest neutron sources tend to be spallation based as high flux fission reactors have an upper bound of neutrons produced. Currently the European Spallation Source in Lund, Sweden is under construction to become the world's strongest intermediate duration pulsed neutron source. Subcritical nuclear fission reactors are proposed to use spallation neutron sources and can be used both for nuclear transmutation and for power generation as the energy required to produce one spallation neutron (~30 MeV at current technology levels) is almost an order of magnitude lower than the energy released by fission (~200 MeV for most fissile actinides).^[9]

Use of neutrons requires high effort and is only feasible at large scale facilities. For most neutron scattering applications neutrons are produced in research facilities by means of fission (in research reactors) or spallation (in accelerator- driven spallation neutron sources). Today there are some 37 neutron sources in 21 countries; of these, 23 are in continental Europe (including Russia and Scandinavia), 9 are in North America (including Canada; IPNS closed in 2008), 2 are in Japan with 1 in each of Australia and India. Five of the sources are spallation sources, the remainder are generally rather aging reactors, though some, such as the ILL, have undergone recent refurbishment to extend their useful lifetimes. The total number of SANS instruments at these sources is 36; of which 21 are to be found at the European facilities. Despite this apparent glut of facilities and instruments, the demand for SANS beam time typically outstrips the beam time actually available by a factor of 2 or 3.^[11]

2 X-rays

An X-ray is a type of high-energy electromagnetic radiation that penetrates the body. The wavelength of most X-rays ranges from 10 picometers to 10 nanometers, corresponding to frequencies ranging from 30×10^{15} Hz to 30×10^{18} Hz and energies ranging from 145 eV to 124 keV. Photo-absorption, Compton scattering, and Rayleigh scattering are the three main ways that X-rays interact with matter. The strength of these interactions is determined by the X-ray energy and the elemental composition of the material.^[6]

Every time charged particles strike a material with enough energy, X-rays are created. An X-ray tube, a vacuum tube that uses a high voltage to accelerate the electrons emitted by a hot cathode to a high velocity, is one of many sources of X-rays.^[6] X-rays can also be produced by fast protons or other positive ions. The proton-induced X-ray emission or particle-induced X-ray emission is widely used as an analytical procedure.^[7] Two other X-ray sources are Synchrotron and Cyclotron.^[8]

2.1 SAXS Small Angle X-rays Scattering

Small angle scattering (SAS) is the collective name given to the techniques of small angle neutron (SANS), X-ray (SAXS) and light (SALS, or just LS) scattering. In each of these techniques radiation is elastically scattered by a sample and the resulting scattering pattern is analysed to provide information about the size, shape and orientation of some component of the sample.^[12]

SAXS is an analytical characterization tool used to determine the structure of particle systems in terms of averaged sizes or shapes. The materials can be solid or liquid and they can contain solid, liquid or gaseous domains of the same or another material in any combination. The method is accurate, non-destructive and usually requires only a minimum of sample preparation. Applications are very broad and include the metal, cement, oil, polymer, plastics, food and pharmaceutical industries and can be found in research as well as in quality control.

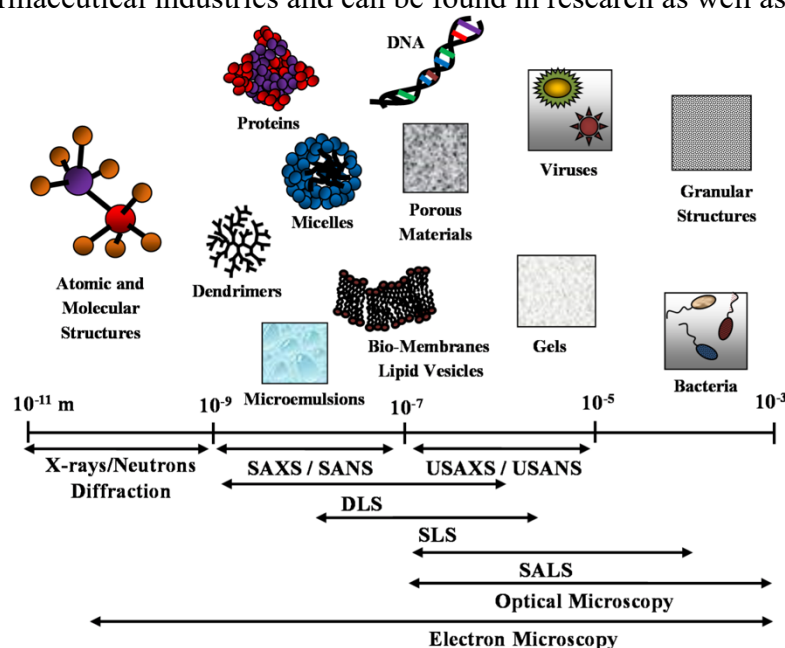


FIG 2. Different space resolution of the main scattering techniques: small angle X-rays and neutrons scattering (SAXS and SANS), ultra-SAXS and ultra-SANS (USAXS and USANS) and dynamic, static and small angle light scattering (DLS, SLS and SALS). Comparison with complementary optical and electron microscopy techniques.^[12]

Small-angle X-ray scattering (SAXS) is an analytical technique that measures the intensities of X-rays scattered by a sample as a function of the scattering angle. Measurements are made at very small angles, typically in the range of 0.1 deg to 5 deg.

From Bragg's law it is understood that with decreasing scattering angle, increasingly larger structural features are being probed. A SAXS signal is observed whenever a material contains structural features on the length scale of nano-meters, typically in the range of 1-100 nm. On the other hand, wide-angle X-ray scattering (WAXS), also known as wide-angle X-ray diffraction (WAXD), probes for structures in the material on the much smaller length scale,

that of interatomic distances. Small angle X-ray scattering and wide angle X-ray scattering (SAXS and WAXS) are complementary techniques.

The experimental setup for SAXS measurements uses a transmission geometry. X-ray optics that create a very narrow, yet highly intense incident X-ray beam are essential. This is because the comparatively weak scattering signal from the sample has to be measured in the immediate vicinity of the direct beam. It is also essential to use a detector which has a high linearity, a high dynamic range and negligible intrinsic noise. A high spatial resolution of the detector is beneficial for high-end SAXS instrumentation, because it allows a good low-angle resolution to be achieved even with a compact experimental setup.

The scattering of X rays by matter is determined almost entirely by the interaction of incident radiation with electrons. A part of nuclear scattering is negligible in that the mass of the nuclei is more than 10³ times greater than the electron mass and the nuclear scattering energy is accordingly 10⁶ times less than the electron scattering energy. For a plane monochromatic incident wave ^[13]

$$E = E_0 \exp[i(k_0 r - \omega t)] \quad 3$$

where E represents the electric field intensity. Amplitude of the scattered wave can be expressed as:

$$E_S = - E_0 \frac{e^2}{mc^2} \frac{1}{r} \sin\psi \quad 4$$

Where e and m are the charge and mass of the electron, c is the velocity of light, r is the distance from the electron to the point of observation and ψ is the angle between the scattering beam and the direction of acceleration of the electron. The phase of scattered radiation relative to the phase of the incident beam changes by 180°.

X-ray scattering length of a single electron is:

$$b_x = \frac{e^2}{mc^2} \sin\psi = r_0 \sin\psi \quad 5$$

where r_0 is Thomson electron radius. Scattering intensity is equal:

$$i_x = b_x^2 = (r_0 \sin\psi)^2 \quad 6$$

For small-angle scattering, where $\psi=90^\circ$,

$$i_x = r_0^2 = 7.95 \times 10^{-25} \text{ cm}^2 \quad 7$$

Integral cross section, which represents total scattering energy scattered by a single electron gives the following value:

$$\sigma_x = \frac{8\pi}{3} r_0^2 = 6.66 \times 10^{-25} \text{ cm}^2 \quad 8$$

In the case of an atom containing Z electrons, electron density is introduced, $\rho_a(r)$, and represents the time averaged probability of the electron distribution in an atom and may be accepted as a spherically symmetric function for free atoms. The scattering length in this case equals:

$$f_a(s) = r_0 L(\theta) \int_0^\infty \rho_a(r) \frac{\sin(sr)}{sr} 4\pi r^2 dr \quad 9$$

Where $L(\theta)$ is the polarization factor. For small-angle scattering studies, the scattering length of an atom is just $f = r_0 Z$ because polarization factor is equal to 1 and integral value is equal to the number of electrons. These relationships are valid when the frequency of incident radiation is much greater than frequency corresponding to the energy excitation of K, L and other shells of the atom. Then, dispersion corrections for scattering length are necessary to include.^[13]

3. SANS Small Angle Neutron Scattering

Neutron scattering is a powerful tool for studying structure and dynamics of matter over a wide range of length- and time-scales. Properties of neutrons, such as electrical neutrality, magnetic moment, and quasi-random variation of the scattering power as a function of atomic number, make it an ideal probe for many areas in modern physics, chemistry, and biology. Neutron scattering allows scientists to count scattered neutrons, measure their energies and the angles at which they scatter, and map their final positions. This information can reveal the molecular and magnetic structure and behaviour of materials, such as high-temperature superconductors, polymers, metals, and biological samples. In addition to studies focused on fundamental physics, neutron scattering research has applications in structural biology and biotechnology, magnetism and superconductivity, chemical and engineering materials, nanotechnology, complex fluids, and others.^[14-15]

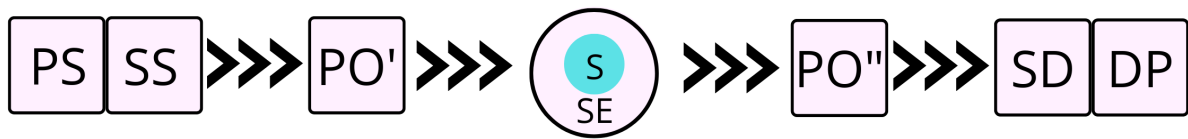


FIG 3. Generic Representation of a neutron scattering experiment; PS = primary source, SS = spectrum shifter, PO = selective phase space operator, SE = sample space, S = sample, SD = signal detector, DP = data processing^[15]

Small-angle scattering of neutron (SANS) and X-rays (SAXS) probe the statistical ensemble of the nano-structures and deal with the diffusion of electromagnetic or particle waves by heterogeneities in matter. An example of a typical scattering geometry is reported in Figure 4. In a small-angle scattering (SAS) experiment, a collimated, monochromatic beam of the incident radiation impinges on a scattering cell (highlighted volume) containing the sample under investigation. The scattering intensity at various scattering angles θ is collected by a detector, placed at a given distance from the sample. The detector is shielded from the primary

beam by an active beam stop, which records the transmitted beam intensity for later use in normalization procedures. The difference between the scattered (k_F) and incident (k_0) wavevectors furnishes the scattering wavevector $q = |k_F - k_0| = (4\pi/\lambda)\sin(\theta)$, which has the dimensions of a reciprocal length (common units are \AA^{-1} or nm^{-1}).^[11]

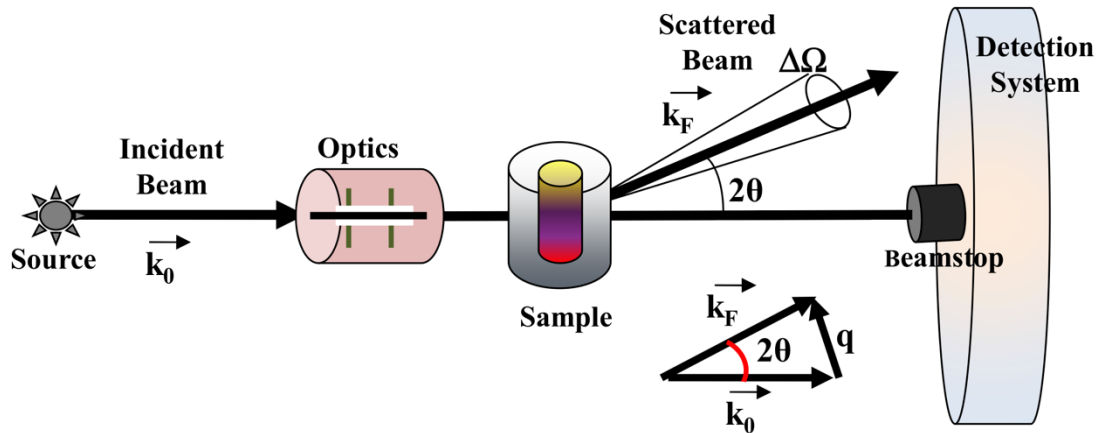


FIG 4. Typical scattering geometry for small angle scattering (SAS) experiments. An incident radiation beam from a neutrons or X-rays source impinging on the material system (sample) under investigation is scattered at a given scattering angle 2θ and is collected by a proper detection system.^[12]

Contrary to X rays, neutrons are not scattered appreciably by electrons. Neutron scattering experiments measure the number of neutrons scattered by a sample as a function of the wavevector change (Q) and the energy change (E) of the neutron. They interact mainly with the nucleus. Wavelength of neutrons is determined by equation $\lambda = h/mv$ where m and v are mass and velocity of neutron and h is the Planck constant. When the neutron beam passes through the moderator at temperature T , the mean-square velocity of the neutrons v^2 satisfies the relationship^[13]

$$mv^2/2 = 3k_B T/2 \quad 10$$

k_B is the Boltzmann constant. The maximum intensity of the thermal neutron spectrum is at wave length :

$$\lambda_{\max} = (h^2/3mk_B T)^{1/2} \quad 11$$

Dimensions of the nucleus are much smaller than the neutron wavelength so the scattering length for thermal neutrons will be isotropic independent of the scattering angle and given by a constant real value over wide energy range, bn , which consist of two parts: potential scattering and resonance scattering. Contrary to the X-ray scattering length it can be either positive or negative sign, depending on the contribution of the two terms in expression.^[13]

3.1 Neutron time-of-flight scattering

In neutron time-of-flight scattering, a form of inelastic neutron scattering, the initial position and velocity of a pulse of neutrons is fixed, and their final position and the time after the pulse that the neutrons are detected are measured. By the principle of conservation of momentum, these pairs of coordinates may be transformed into momenta and energies for the neutrons, and the experimentalist may use this information to calculate the momentum and energy transferred to the sample. Inverse geometry spectrometers are also possible. In this case, the final position and velocity are fixed, and the incident coordinates varied. The Time-of-flight Method Uses Multiple Wavelength Slices at a Reactor or a Pulsed Spallation Source.^[16]

The Neutron Time Of Flight (n-TOF) facility is a neutron spectrometer at CERN. It consists of a pulsed source, a flight path of 200 m length, and a detector systems. Neutron energies are deduced from the time of flight between source and detector; hence the name of the facility. The neutrons are produced by neutron spallation; by directing a pulsed beam of protons from the Proton Synchrotron (PS) towards a lead target about 300 neutrons expelled for each impact of a proton. The neutrons are slowed after being emitted, first by the lead target and afterwards by a slab containing water. This results in a wide range of neutron energies since some neutrons will slow down more than others when passing through the targets. Finally, the neutrons are ejected through the 200m long flight path before they arrive at an experimental area.^[16]

Chapter B. Experimental Work By SasView

1. SasView Software

SasView^[17] software is an open source, collaboratively developed software for the analysis of any small angle scattering data. The software is written in Python with C and C++ modules providing some of the heavier computations.

SasView was originally developed by the University of Tennessee as part of the Distributed Data Analysis of Neutron Scattering Experiments (DANSE) project funded by the US National Science Foundation (NSF) but is currently being developed as an Open Source project hosted on GitHub and managed by a consortium of scattering facilities. Participating facilities include (in alphabetical order): the Australian National Science & Technology Centre for Neutron Scattering, the Diamond Light Source, the European Spallation Source, the Federal Institute for Materials Research and Testing, the Institut Laue Langevin, the ISIS Pulsed Neutron & Muon Source, the National Institute of Standards & Technology Centre for Neutron Research, the Oak Ridge National Laboratory Neutron Sciences Directorate, and the Technical University Delft Reactor Institute.

SAS analysis is a fairly broad term, potentially covering a huge amount of ground and often meaning different things to different people. As part of this project several boundaries were identified and defined. The first boundary is the distinction between SAS reduction and

SAS analysis. Reduction is defined as the process that removes all instrument specific “artefacts” and produces a reduced data set containing only the “science” of the material being investigated. If done perfectly reduced data from any instrument should lie on top of one another with minor caveats regarding differences in the contrast term arising out of the use of different types of radiation. The rationale is that every instrument is different and every source is different. Thus reduction will always be a process relatively unique to the instrument on which the data was taken and only the facilities’ instrument scientists are truly qualified to know what all those details are. By contrast, once in reduced form, the job of the user scientist can begin in earnest as that is the data that contains the information he/she is seeking. Further, at this point the “analysis” problem becomes a completely common and generic problem so that all facilities and the community at large can easily collaborate having now the exact same needs. SasView is designed to operate on reduced data and thus should be instrument agnostic.

The second demarcation is between real space and inverse space analysis. By inverse space analysis we mean the process of thinking about data in inverse space as collected, while by real space analysis we mean the process of thinking about the data in real 3D space. The first case represents the traditional approach to SAS analysis used by colloid and materials scientists while the second has been pioneered mostly by the biological scattering community. We believe that these are two very different ways of thinking about the problem and it would be very difficult to create a single user interface ideal for both. Thus SasView is designed as an inverse space modelling tool. We hope to build partnerships to interact with real space analysis packages such as the SASSIE project, providing if appropriate support in making them relevant beyond biological systems. Two methods cross this boundary: Distance distribution, $P(R)$, and correlation function analyses which attempt a direct inversion of the data to real space with no a priori assumptions, and shape reconstruction or “ab initio” methods which seek to refine an arbitrary 3D real space model till its Fourier inversion fits the scattering data.

SasView supports the canSAS 1D XML file format, but will read almost any 1D ASCII column data (but not any associated metadata). For 2D data SasView reads the newly-ratified canSAS 2D NeXus HDF5 format in addition to the NIST 2D ASCII format. SasView was developed with a view to take advantage of modern computing power to make analysis of non-azimuthally symmetric 2D data (such as obtained under the influence of a directional field such as flow, or magnetic or electric fields) more routine.

1.1 Features of SasView software

Different Type of analysis can be performed using SasView

Fitting

Performs optimized model-fitting on one or more datasets, with or without constraints, polydispersity or orientation distributions, or resolution smearing.

SasView can fit data in one of three ways:

- Single fit mode - individual data sets are fitted independently one-by-one
- Simultaneous fit mode - multiple data sets are fitted simultaneously to the same model with/without constrained parameters (this might be useful, for example, if you have measured the same sample at different contrasts)
- Batch fit mode - multiple data sets are fitted sequentially to the same model (this might be useful, for example, if you have performed a kinetic or time-resolved experiment and have lots of data sets).

Pr Inversion

This tool calculates a real-space distance distribution function, $P(r)$ for a dataset, using the inversion approach. $P(r)$ inversion requires that the background be perfectly subtracted. This is often difficult to do well and thus many data sets will include a background. For those cases, the user should check the “Estimate background level” option and the module will do its best to estimate it. If you know the background value for your data, select the “Input manual background level” option.^[18]

Invariant

Calculates the Porod Invariant or ‘Total Scattering’ for a dataset. For any multi-phase system, i.e. any system that contains regions with different scattering length densities (SLD), the integral over all of the appropriately dimensionally-weighted scattering cross-section i.e intensity is a constant directly proportional to the mean-square average fluctuation in SLD and the phase composition. Usefully, this value is independent of the sizes, shapes, or interactions, or, more generally, the arrangement, of the phase domains (i.e. it is **invariant**) provided the system is incompressible.

As the invariant is a fundamental law of scattering, it can be used for sanity checks (for example, scattering patterns from the same sample that may look very different should have the same invariant if the hypothesis of what is going on in the sample is correct), to cross-calibrate different SAS instruments.^[19]

Correlation Function

Calculates the 1D density correlation function for a dataset. If the data is from a sample that can be described by idealized lamellar morphology this analysis will also attempt to extract some morphological information from the correlation function, eg, lamellar spacing, crystallinity, etc.

2. Example 1

2.1 Fitting with Levenberg-Marquardt and Dream algorithm

Example studied : ISIS_Polymer_Blend_RT2 (mixture of h8 - polystyrene and d8 - polystyrene)

To begin with, we have to start the application SasView. Then, from the Data Explorer panel we load the data we want to analyse, so we choose from the folder \test\1d_data the intended compound, which in our case is ISIS_Polymer_Blend_RT2.xml dataset and press open. Here upon, from the Data Explorer we select the option Fitting and Send data to begin the process of fitting.

In the Fit Page, select the model Category called **shape-independent** and then from the drop-down box below select the **mono_gauss_coil** model. Click the Show Plot button.

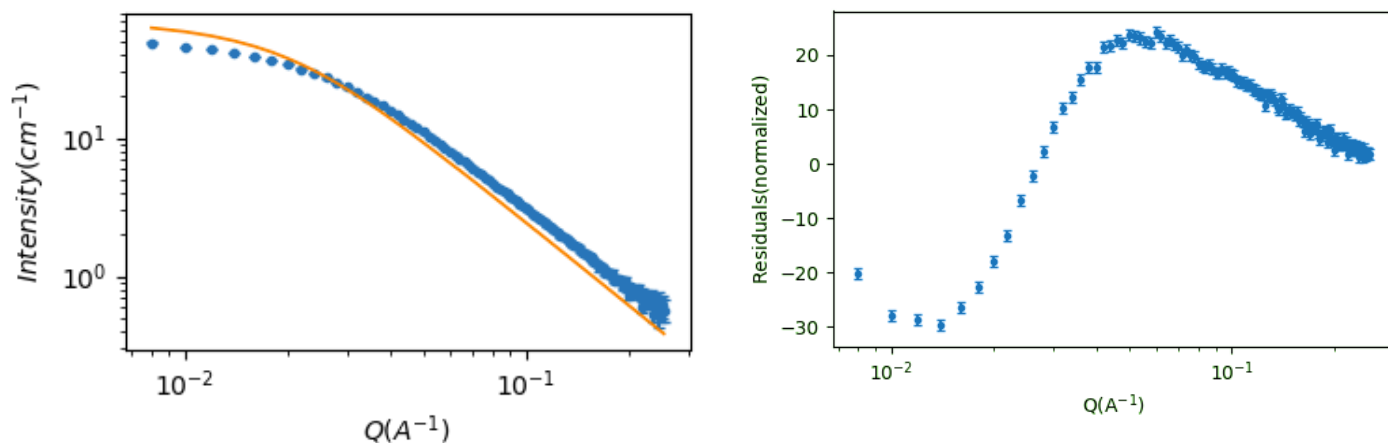


FIG 5. Plots of Intensity-Q and Residuals(normalized)-Q for the compound **ISIS_Polymer_Blend_RT2** with $X^2=192.83$

mono_gauss_coil^[20]

Scattering from monodisperse polymer coils. This Debye Gaussian coil model strictly describes the scattering from *monodisperse* polymer chains in theta solvents or polymer melts, conditions under which the distances between segments follow a Gaussian distribution.

The returned value is scaled to units of $\text{cm}^{-1} \text{sr}^{-1}$, absolute scale.

$$I(q) = \text{scale} \cdot I_0 \cdot P(q) + \text{background}$$

$$I_0 = \varphi_{\text{poly}} \cdot V \cdot (\rho_{\text{poly}} - \rho_{\text{sol}})^2 \quad P(q) = 2[\exp(-Z) + Z - 1]/Z^2$$

$$Z = (qR_g)^2$$
$$V = M/(NA\delta)$$

Here, φ_{poly} is the volume fraction of polymer, V is the volume of a polymer coil, M is the molecular weight of the polymer, N_A is Avogadro's Number, δ is the bulk density of the polymer, ρ_{poly} is the sld of the polymer, ρ_{solv} is the sld of the solvent, and R_g is the radius of gyration of the polymer coil.

The 2D scattering intensity is calculated in the same way as the 1D, but where the q vector is redefined as

$$q = \sqrt{q_x^2 + q_y^2}$$

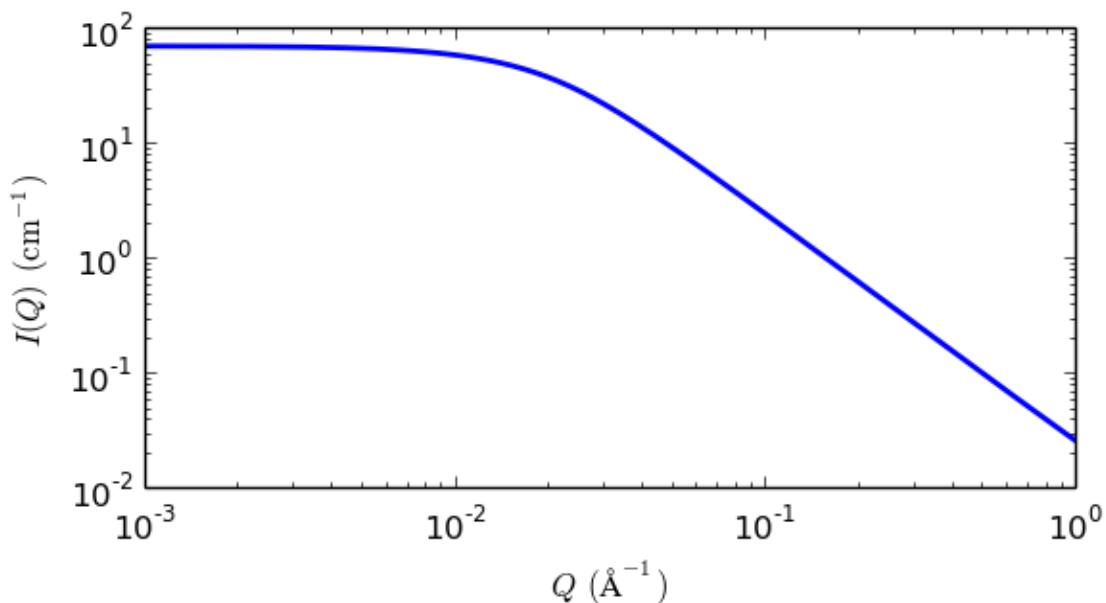


FIG 6. 1D plot corresponding to the default parameters of the model.

Looking at the upper graph, it is clear that the statistical quality of the measured data degrades at higher-Q values. We can exclude these points from the fitting using the Q range. set the maximum-Q value to 0.19 Å⁻¹.

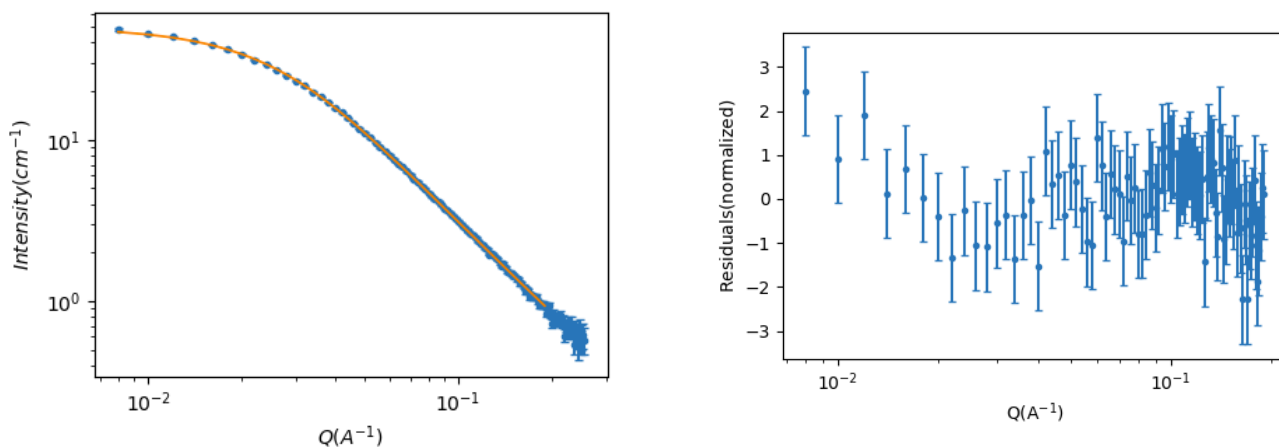
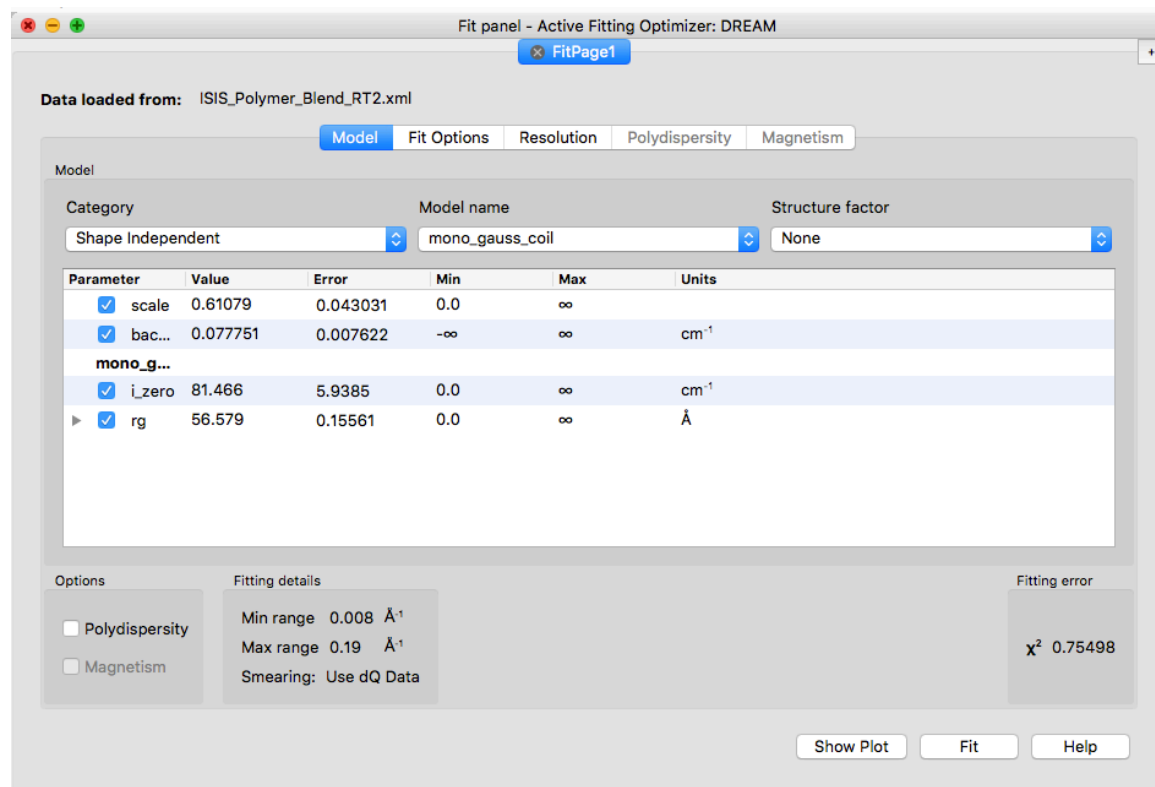


FIG 7. Plots of Intensity-Q and Residuals(normalized)-Q for the compound **ISIS_Polymer_Blend_RT2** with $X^2=0.7893$

2.2 Using Dream Algorithm

The default optimiser, called the Levenberg-Marquardt, is a fast optimiser, but is prone to finding what are called 'local solutions' in parameter-space, rather than the true 'global solution'. More robust optimisers will be more likely to find the 'global solution' but will be slower. The most robust optimiser in SasView is the one called DREAM.



Go to the Menu Bar and click Fitting followed by Fit Algorithms. Then select DREAM from the drop-down list of algorithms and click Ok. Return to the Fit page and click Fit. When the fit has completed, go to the Menu Bar and click Fitting and then select Fit Results. It is also evident that DREAM has been able to improve the solution: χ^2 .

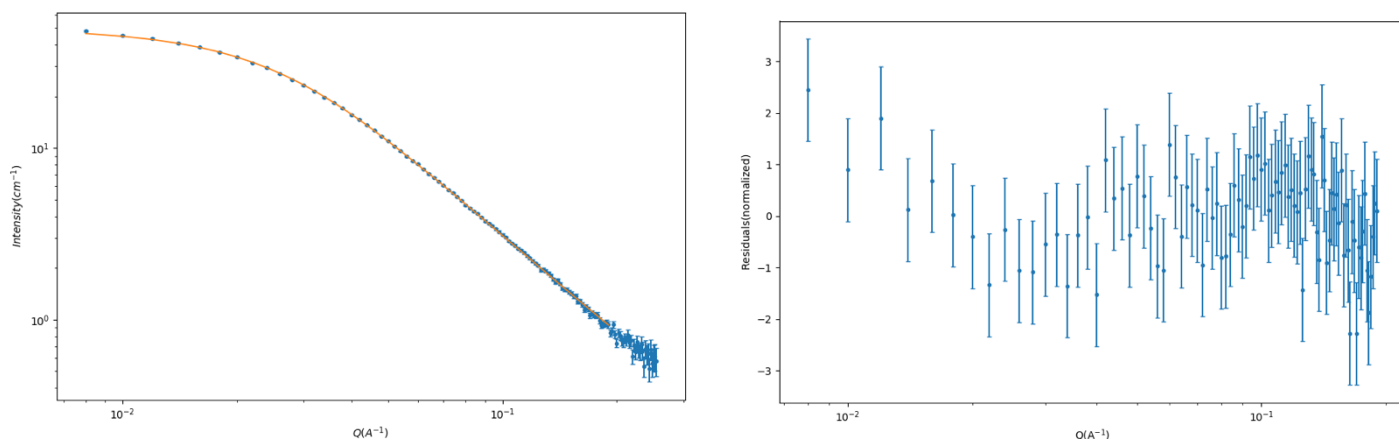


Fig 8. Plots of Intensity-Q and Residuals(normalized)-Q for the compound **ISIS_Polymer_Blend_RT2** with $\chi^2=0.75498$

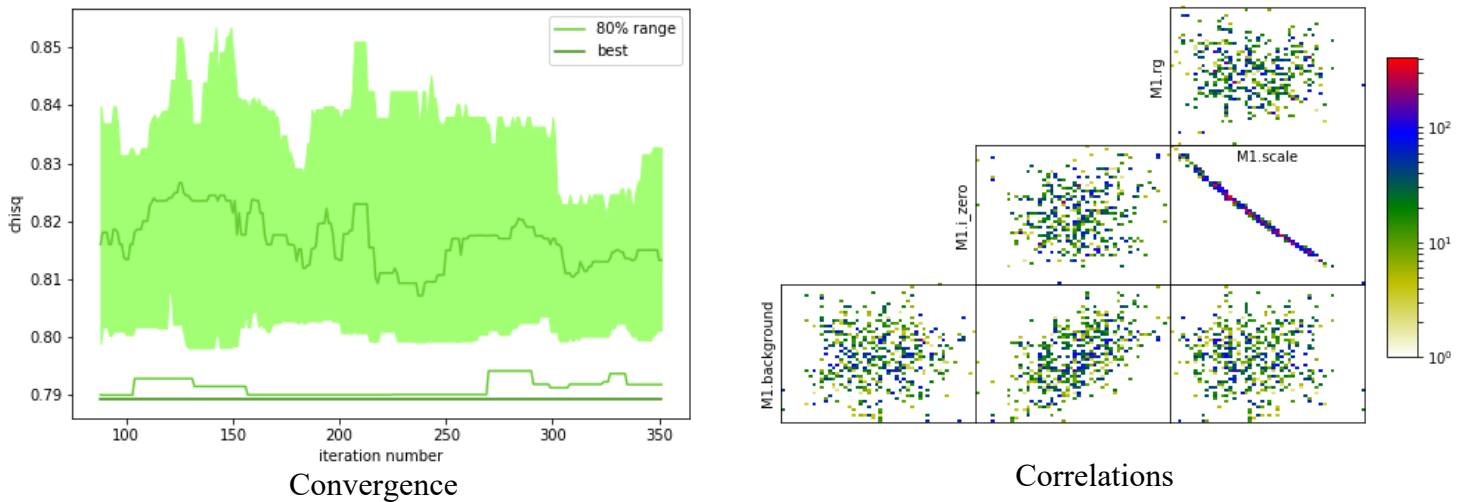


FIG 9. Fitting Results obtained by Dream Algorithm

3. Example 2 : Correlation Function Analysis

Sample Used : ISIS_98929 : nylon-6 (polyamide-6) hydrated with heavy water(D20).

Select the ISIS_98929.txt dataset and click the Open button. Nylon is a semi-crystalline polymer, meaning it is composed of alternating regions of crystalline (more dense) and amorphous (less dense) polymer. When hydrated, water molecules preferentially locate to the amorphous regions. If heavy water is used the SLD of the amorphous regions is enhanced relative to the SLD of the crystalline regions.

At the bottom of the Data Explorer panel, click the drop-down that currently says 'Fitting' and select . Then click the Send To button.

The three bars represent the limits of the measured data that will be used to construct the extrapolation functions. In the case of the low-Q extrapolation, all data to the left of

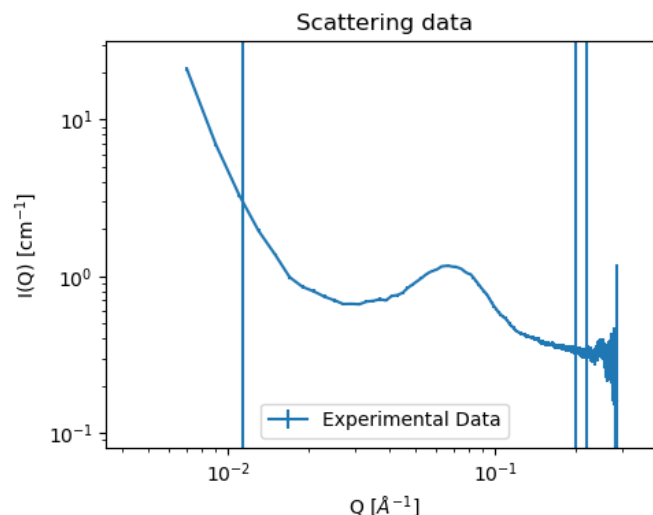


FIG 10. Scattering Data Plot of ISIS_98929.

the leftmost blue vertical bar is used. In the case of the high-Q extrapolation, data between the two rightmost blue vertical bars is used.

Then Calculate Background and Extrapolation Parameters by clicking on background button followed by Extrapolate. And finally get the output by clicking Extract Parameters.

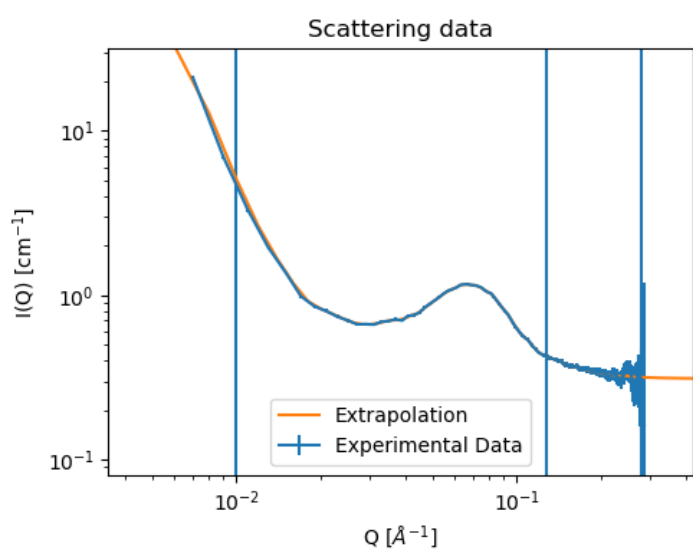


FIG 11. ISIS_98929 scattering Data Plot with Extrapolation

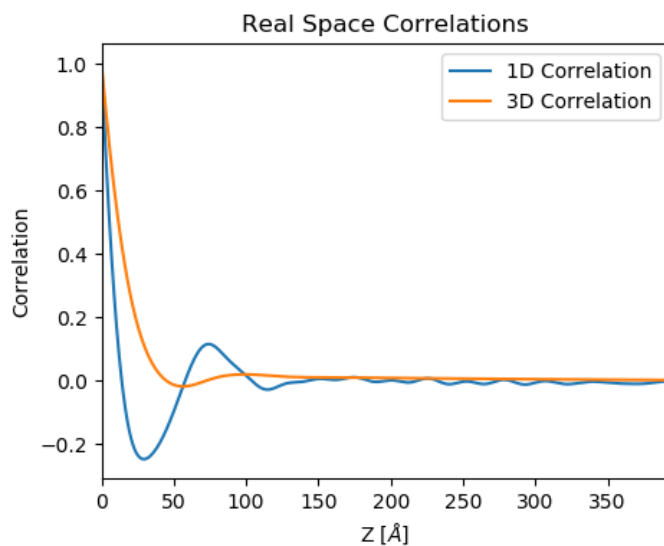


FIG 12. Real Space Correlations Transform

Background

background

Extrapolation parameters

Guinier Porod

A
 K

B
 σ

Output parameters

Long Period

Average Hard Block Thickness

Polydispersity

Average Interface Thickness

Average Core Thickness

Local Crystallinity

FIG 13. Background, Extrapolation Parameters and output Parameters obtained after calculations.

4. Example 3. P_New [SANS]

The model used for fitting the P_New.sans. file is "spinodal" with fitting error $\chi^2 = 4.515$.

The scattering intensity $I(q)$ is calculated as

$$I(q) = I_{max} \frac{(1 + \gamma/2)x^2}{\gamma/2 + x^{2+\gamma}} + B$$

where $x=q/q_0$, q_0 is the peak position, I_{max} is the intensity at q_0 (parameterised as the scale parameter), and B is a flat background. The spinodal wavelength, Λ , is given by $2\pi/q_0$.

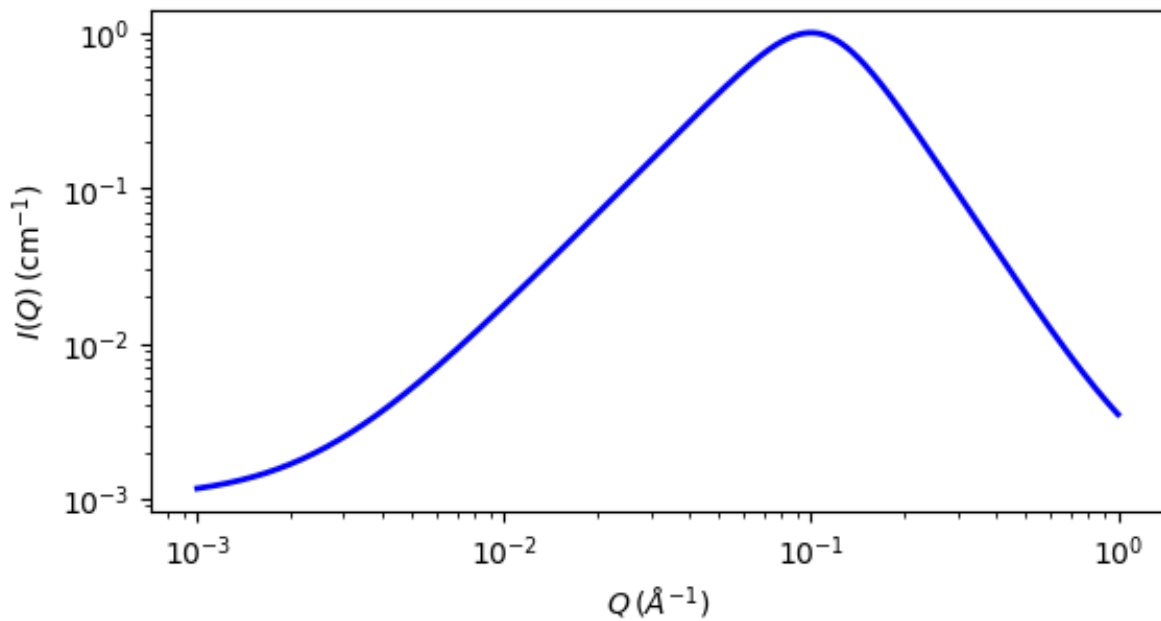


FIG 14. 1D plot corresponding to the default parameters of the model.

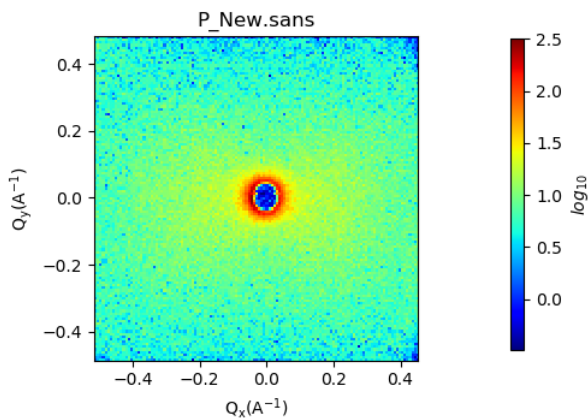


FIG 15. Experimental Data

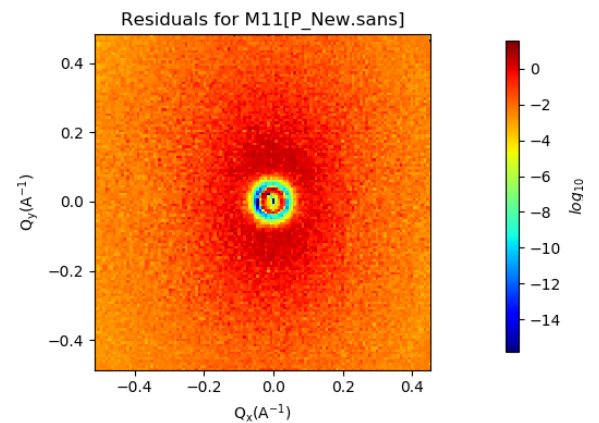


FIG 16. Residual Portion after Treatment

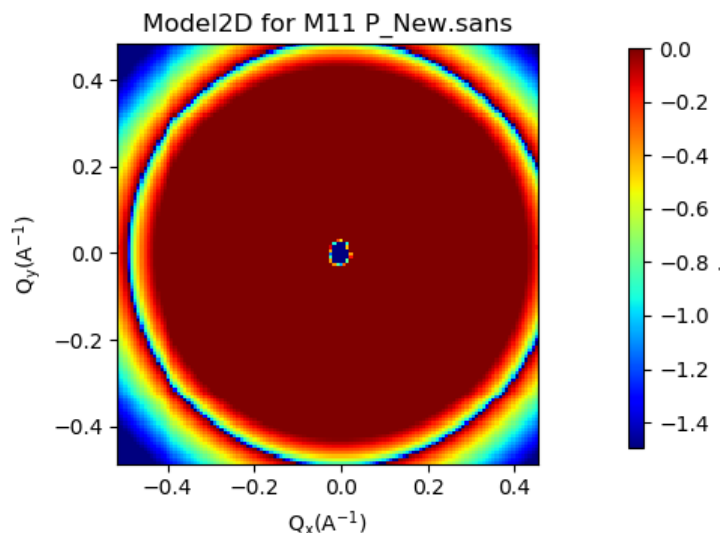


FIG 17. Modelled Result

The following table shows the parameters of SasView used to produce the figures above:

Parameter	Description	Units	Default value	Error
scale	Scale factor or Volume fraction	None	28.475	0.1458
background	Source background	cm^{-1}	-5.0688	0.0847
gamma	Exponent	None	1.307	0.0136
q_0	Correlation peak position	\AA^{-1}	0.090597	0.000427

Table 1: Fit Panel and Model Details

Inferentially, we loaded a compound to the Fit page and we started setting the parameters in order to achieve a better fitting. With the setting of the appropriate model i.e. spinodal in this case, we reduced the chi-square and we reached it very close to the desired value, which is 1.

In my initial attempts I assumed different models (Lorentz guinier, star_polymer) and the X^2 came to 7.9377, but in the last one we assumed the spinodal model and achieved a fitting error of 4.515. It is a fact that we should have more meticulous measurements and higher quality data for the purpose of acquiring better knowledge and clear view of the models.

References

- [1] W. Bothe, H. Becker, Künstliche Erregung von Kern- γ -Strahlen (Artificial excitation of nuclear γ rays), *Z. Phys.* 66 (1930) 289.
- [2] I. Curie, Sur le rayonnement γ nucléaire excité dans le glucinium et dans le lithium par les rayons α du polonium, *C. r. hebd. séances Acad. sci. Paris*, 193 (1930) 1412 (glucinium is an old synonym of beryllium).
- [3] F. Joliot, Sur l'excitation des rayons γ nucléaires du bore par les particules α . Énergie quantique du rayonnement γ du polonium, *C. r. hebd. Séances, Acad. sci. Paris* 193 (1931) 1415.
- [4] J. Chadwick, The Existence of Neutron, 1932 *Nature* 692-708.
- [5] Hartmut Abele, The neutron. Its properties and basic interactions, *Progress in Particle and Nuclear Physics*, Volume 60, Issue 1, 2008, Pages 1-81, SSN 0146-6410, <https://doi.org/10.1016/j.pnpnp.2007.05.002>.
- [6] Tafti D, Maani CV. X-ray Production. In: StatPearls [Internet]. Treasure Island (FL): StatPearls Publishing; 2022 Jan-. Available from: <https://www.ncbi.nlm.nih.gov/books/NBK537046/>
- [7] Whaites, Eric; Cawson, Roderick (2002). *Essentials of Dental Radiography and Radiology*. Elsevier Health Sciences. pp. 15–20. ISBN 978-0-443-07027-3.
- [8] Paul, Helmut; Muhr, Johannes (1986). "Review of experimental cross sections for K-shell ionization by light ions". *Physics Reports*. 135 (2): 47–97. Bibcode:1986PhR...135...47P. doi:10.1016/0370-1573(86)90149-3.
- [9] Valery Nesvizhevsky, Jacques Villain, The discovery of the neutron and its consequences (1930–1940), *Comptes Rendus Physique*, Volume 18, Issues 9–10, 2017, Pages 592-600, ISSN 1631-0705, <https://doi.org/10.1016/j.crhy.2017.11.001>.
- [10] Andrew Taylor and Mike Dunne and Steve Bennington and Stuart Ansell and Ian Gardner and Peter Norreys and Tim Broome and David Findlay and Richard Nelves, A Route to the Brightest Possible Neutron Source , *Science*, 315, 1092-1095, 2007, doi.10.1126/science.1127185
- [11] Stephen M. King, *Small Angle Neutron Scattering*, Large-Scale Structures Group ISIS Facility, STFC Rutherford Appleton Laboratory Harwell Oxford, Didcot, OX11 0QX United Kingdom December 1995 (Revised Oct 2013)

- [12] Lombardo, D.; Calandra, P.; Kiselev, M.A. Structural Characterization of Biomaterials by Means of Small Angle X-rays and Neutron Scattering (SAXS and SANS), and Light Scattering Experiments. *Molecules* 2020, 25, 5624. <https://doi.org/10.3390/molecules25235624>
- [13] Feigin, L.A.; Svergun, D.I. Structure Analysis by Small-Angle X-ray and Neutron Scattering; Plenum Press: New York, NY, USA; Springer: London, UK, 1987. <https://doi.org/10.1002/actp.1989.010400317>
- [14] P. Smeibidl et al., "First Hybrid Magnet for Neutron Scattering at Helmholtz-Zentrum Berlin," in *IEEE Transactions on Applied Superconductivity*, vol. 26, no. 4, pp. 1-6, June 2016, Art no. 4301606, doi: 10.1109/TASC.2016.2525773.
- [15] Squires, G L. Introduction to the Theory of Thermal Neutron Scattering. Cambridge: Cambridge University Press, 2012. Print.
- [16] E. Mamontov and K. W. Herwig, "A time-of-flight backscattering spectrometer at the Spallation Neutron Source, BASIS", *Review of Scientific Instruments* 82, 085109 (2011) <https://doi.org/10.1063/1.3626214>.
- [17] M. Doucet et al. SasView Version 5.0.3, Zenodo, 10.5281/zenodo.3930098
- [18] P.B. Moore *J. Appl. Cryst.*, 13 (1980) 168-175
- [19] Y.B. Melnichenko Chapter 6 in *Small-Angle Scattering from Confined and Interfacial Fluids*; Springer, 2016.
- [20] R J Roe, *Methods of X-Ray and Neutron Scattering in Polymer Science*, Oxford University Press, New York (2000).